PHYSICAL REVIEW C **77**, 061303(R) (2008)

Proton-proton correlations observed in two-proton decay of ^{19}Mg and ^{16}Ne

I. Mukha,[1,2] L. Grigorenko,[3,4] K. Sümmerer,[4] L. Acosta,[5] M. A. G. Alvarez,[1] E. Casarejos,[6] A. Chatillon,[4] D. Cortina-Gil,[6] J. M. Espino,[1] A. Fomichev,[3] J. E. García-Ramos,[5] H. Geissel,[4] J. Gómez-Camacho,[1] J. Hofmann,[4] O. Kiselev,[4,7,8] A. Korsheninnikov,[2] N. Kurz,[4] Yu. Litvinov,[4] I. Martel,[5] C. Nociforo,[4] W. Ott,[4] M. Pfützner,[9] C. Rodríguez-Tajes,[6] E. Roeckl,[4] M. Stanoiu,[4,10] H. Weick,[4] and P. J. Woods[11]

[1]*Universidad de Sevilla, E-41012 Seville, Spain*
[2]*RRC "Kurchatov Institute", RU-123184 Moscow, Russia*
[3]*Joint Institute for Nuclear Research, RU-141980 Dubna, Russia*
[4]*Gesellschaft für Schwerionenforschung, D-64291 Darmstadt, Germany*
[5]*Universidad de Huelva, E-21071 Huelva, Spain*
[6]*Universidade de Santiago de Compostela, E-15782 Santiago de Compostela, Spain*
[7]*Johannes Gutenberg Universität, D-55099 Mainz, Germany*
[8]*Paul Scherrer Institut, CH-5232 Villigen, Switzerland*
[9]*IEP, Warsaw University, PL-00681 Warszawa, Poland*
[10]*IFIN-HH, P.O. Box MG-6, Bucharest, Romania*
[11]*University of Edinburgh, EH1 1HT Edinburgh, United Kingdom*

(Received 4 February 2008; published 13 June 2008)

Proton-proton correlations were observed for the two-proton decays of the ground states of ^{19}Mg and ^{16}Ne. The trajectories of the respective decay products, $^{17}\mathrm{Ne} + p + p$ and $^{14}\mathrm{O} + p + p$, were measured by using a tracking technique with microstrip detectors. These data were used to reconstruct the angular correlations of fragments projected on planes transverse to the precursor momenta. The measured three-particle correlations reflect a genuine three-body decay mechanism and allowed us to obtain spectroscopic information on the precursors with valence protons in the *sd* shell.

DOI: 10.1103/PhysRevC.77.061303 PACS number(s): 27.20.+n, 21.10.−k, 21.45.−v, 23.50.+z

Two-proton ($2p$) radioactivity is a specific type of genuine three-particle nuclear decay. It occurs when a resonance in any pair of fragments is located at higher energies than in the initial three-body ($p + p$+"core") nucleus, and thus simultaneous emission of two protons is the only decay channel. The exclusive features of this phenomenon were illuminated by V. I. Goldansky in his classical work [1]. Three-body systems have more degrees of freedom than two-body systems, hence additional observables appear. In the case of $2p$ emission, the energy spectra of single protons become continuous, and proton-proton (p-p) correlations are available, which makes them a promising probe of nuclear structure or/and the decay mechanism. For example, the first p-p correlations observed in the $2p$ radioactivity of ^{94m}Ag revealed strong proton yields in either the same or opposite directions, which called for a theory of $2p$ emission from deformed nuclei [2].

Two-proton emission can also occur from short-lived nuclear resonances or excited states (see, e.g., Refs. [3–5]). Though in this case the mechanism of $2p$ emission may depend on the reaction populating the parent state, such nuclei can be easily studied in flight. For example, the cases of ^{6}Be [3,6] and ^{16}Ne [7] were studied by analyzing their p-p correlations in the framework of a three-body partial-wave analysis developed for three-particle decays of light nuclei. Very recently, p-p correlations were also observed in $2p$ radioactivity of ^{45}Fe, where both the lifetime and p-p correlations were found to reflect the structure of pf-shell $2p$ precursors [8].

In the present paper, we study for the first time the p-p correlations in *sd*-shell nuclei via the examples of the $2p$ decays of ^{19}Mg and ^{16}Ne. These nuclei with very different half-lives ($T_{1/2} \approx 4 \times 10^{-12}$ [9] and $T_{1/2} \approx 4 \times 10^{-19}$ s [10], respectively) and presumably different spectroscopic properties may serve as reference cases for theoretical studies of the nuclear structure of other possible $2p$ emitters with *sd*-wave configurations. The decay properties of states in ^{19}Mg and ^{16}Ne and the related resonances in ^{18}Na and ^{15}F are shown in Fig. 1, which compiles the data from Refs. [9–15] and this work. The ground states of both isotopes decay only by simultaneous $2p$ emission, while their excited states are open for sequential $1p$ decays via intermediate unbound states in ^{18}Na and ^{15}F.

The quantum-mechanical theory of $2p$ radioactivity which uses a three-body model [16–18] predicts the p-p correlations to be strongly influenced by nuclear structure together with Coulomb and three-body centrifugal barriers. The newly discovered $2p$ radioactivity of ^{19}Mg [9] is of special interest. The p-p correlations from the $2p$ decay of ^{19}Mg were predicted to reflect the *sd* configurations of the valence protons [19]. A similar effect is found in ^{16}Ne, where the *s*-wave configuration was predicted to dominate, contrary to its mirror ^{16}C, thus breaking isospin symmetry [20]. A complementary approach in describing $2p$ decays is the mechanism of sequential emission of protons via an intermediate state (see, e.g., Ref. [21]). It includes also the traditional quasiclassical diproton model with emission of a ^{2}He cluster, assuming extremely strong p-p correlations [1,22]. The predictions of these models differ dramatically with respect to the p-p correlations, suggesting them as a sensitive probe of the $2p$-decay mechanism (see the detailed predictions below).

Our experiment to investigate $2p$-emission from ^{19}Mg and ^{16}Ne was performed by using a 591*A* MeV beam of ^{24}Mg

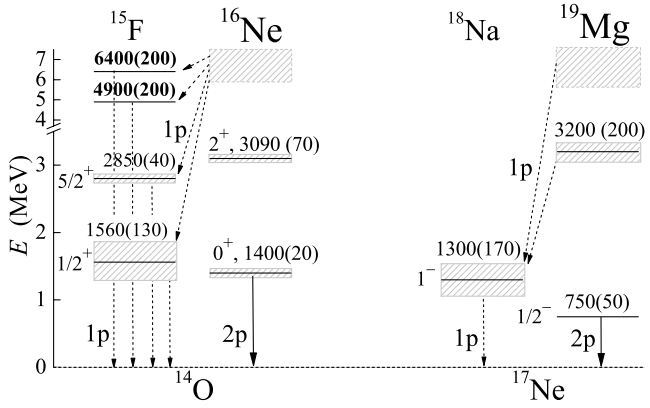

FIG. 1. States observed in ^{16}Ne, ^{19}Mg and the corresponding intermediate systems ^{15}F, ^{18}Na. Decay energies (in keV) are given relative to the respective p and $2p$ thresholds. Most values have been taken from the literature [9–15], those in bold print are from the present work.

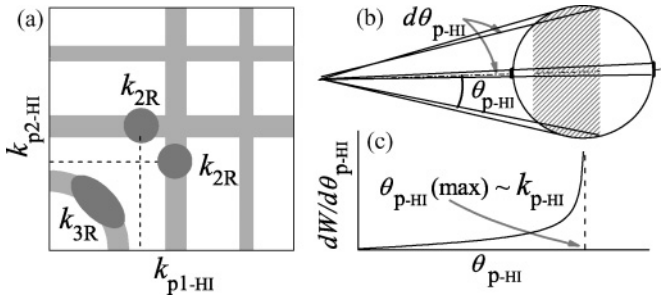

FIG. 2. (a) Cartoon of momentum correlations $k_{p1-\text{HI}}$-$k_{p2-\text{HI}}$ expected for a direct three-body decay (the area k_{3R}) and sequential $2p$ decay (grey boxes with black peaks k_{2R}). (b) Sketch of the kinematic enhancement of an angular p-HI correlation at the maximum possible angle for a given momentum between the decay products. (c) Corresponding angular p-HI distribution.

accelerated by the Schwerionen Synchrotron (SIS) facility at GSI, Darmstadt. The radioactive beams of ^{20}Mg and ^{17}Ne were produced at the projectile-fragment separator (FRS) [23] with average intensities of 400 and 800 ions s^{-1} and energies of 450A and 410A MeV, respectively. The secondary 1-n-removal reactions (^{20}Mg, ^{19}Mg) and (^{17}Ne, ^{16}Ne) occurred at the midplane of the FRS in a secondary 2 g/cm^2 ^{9}Be target. Special magnetic optics settings were applied, the first FRS half being tuned in an achromatic mode using a wedge-shaped degrader, while its second half was set for identification of the heavy ions (HI) with high acceptance in angle and momentum.

A sketch of the experimental setup at the FRS midplane is shown in Fig. 1 of Ref. [9] and explained in detail there. A microstrip detector array (MSD, [24]) consisting of four 7×4 cm^2 double-sided silicon detectors (with a strip pitch of 100 μm), was arranged in three planes positioned 26, 86, and 286 mm downstream from the secondary target. This array was used to measure energy loss and position of coincident hits of two protons and a heavy fragment. Protons fire only one strip of MSD, thus their position uncertainty is $\sigma_x = 100/\sqrt{12} \approx 30$ μm. Ne(Mg) ions produce clusters typically of 7(9) strips wide. Their centroids can be found with uncertainties of $\sim$15 μm as determined from tracking beam ions through three layers of MSD. Proton-HI vertices were defined by distances of closest approach of their respective trajectories within 150 μm. The uncertainty of defining a HI+p + p three-particle vertex in the beam direction depends on the two proton-HI angles (taken from the same HI+p + p event) and varies typically from 0.3 to 1 mm. The angular resolution was mainly due to the angular straggling of the protons in the MSDs and amounted to $\sim$1 mrad. More details concerning the detector performance and tracking procedure are given in Ref. [9]. The heavy $2p$-out residuals (^{17}Ne and ^{14}O) were unambiguously identified by their time of flight, magnetic rigidity, and energy loss measured with the position-sensitive scintillator detectors at the second half of the FRS.

The $2p$ decays of the ground states of ^{19}Mg and ^{16}Ne were identified by using angular correlations between the single protons and their respective cores ^{17}Ne and ^{14}O, which allowed the measurement of the $2p$-decay energies. In general, $2p$ decays may proceed via either sequential or direct decay mechanisms. The first case can be described as two consecutive $1p$ decays through an intermediate resonance [21]. In a schematic two-dimensional (p_1-HI)-(p_2-HI) scatter plot in Fig. 2(a), the first case should populate loci marked by k_{2R}; the widths of the peaks reflect the width of the intermediate state. Sequential proton emission from a single $2p$ parent state via narrow p-HI resonances should yield double peaks, while $2p$ deexcitation of continuum parent states with p-HI final-state interactions should reveal "slices" as shown in Fig. 2(a). In the second case, the simultaneously emitted protons are likely to share the $2p$-decay energy evenly, with both p-HI spectra being identical and peaked at $E/2$ [16,22]. In this case, the area marked k_{3R} in Fig. 2 should be populated, along the arc area with the root-mean-squared proton momentum being constant. In all cases, the patterns in Fig. 2 should by symmetric due to permutation of protons.

Similar structures can be found in the angular $\theta_{p1-\text{HI}}$-$\theta_{p2-\text{HI}}$ correlations for the following reason. As shown schematically in Fig. 2(b), protons emitted isotropically in the $1p$ precursor frame are located in a narrow cone in the laboratory frame due to kinematic forward focusing, with the maximum intensity showing up around the largest possible angle. The p-HI angles reflect the transverse proton momentum relative to the HI one and are therefore correlated with the precursor's decay energy. Thus sequential $2p$ decays from excited states in parent nuclei should be mostly located in peaks with tails along the respective slices in the angular θ_{p1-HI}-θ_{p2-HI} correlations, in analogy to those sketched in Fig. 2(a). In direct $2p$ decays, the single-proton energy spectrum always exhibits a relatively narrow peak centered close to half of the $2p$-decay energy; such energy distribution is a stable feature of this decay mechanism [1,19]. Correspondingly, a bump should appear in the angular correlations in the same way as it should appear along the arc marked by k_{3R} in the scatter plot in Fig. 2. This correspondence between angular and momentum correlations has been used to derive the $2p$-decay energy

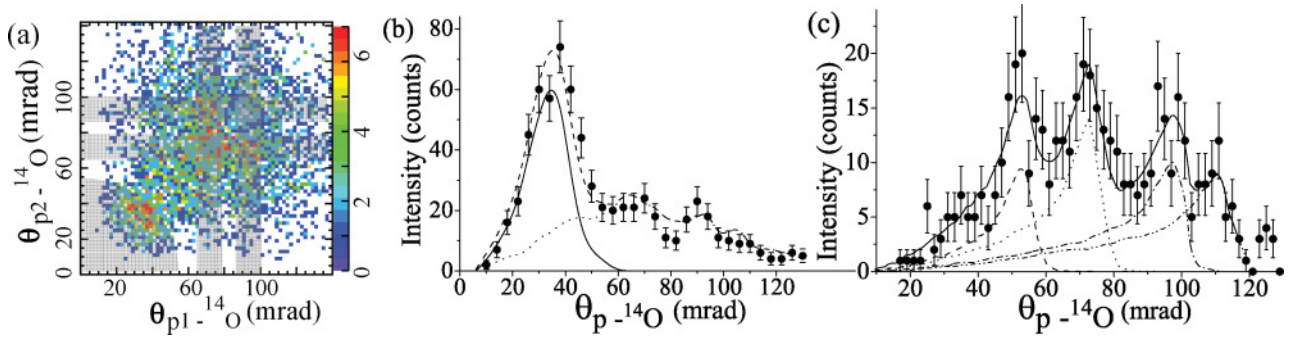

FIG. 3. (Color online) (a) Angular (p_1-^{14}O)-(p_2-^{14}O) correlations obtained from the measured $^{14}O + p + p$ events (colored boxes with scale shown on right). The grey areas indicate simultaneous and sequential $2p$ emission in analogy to those shown in Fig. 2. (b) Angular p-^{14}O distribution (full circles with statistical uncertainties) obtained from the data shown in panel (a) by selecting the other proton angle θ_{p2-O} within the range from 0 to 45 mrad, which corresponds to the ground state of ^{16}Ne. The solid curve represents the Monte Carlo simulation of the detector response for $^{16}\text{Ne}_{gs} \rightarrow {}^{14}O + p + p$ with a $2p$-decay energy of 1.35(8) MeV which agrees with the value of 1.4(1) MeV measured in Ref. [11]. The dashed line is a sum fit to the data. The dotted curve indicates the background as explained in the text. (c) Angular p-^{14}O distribution obtained from the data shown in (a) by selecting the other proton angle from 120 to 150 mrad, which corresponds to p-^{14}O final-state interactions due to the ground and excited states of ^{15}F. The dashed and dotted curves are the Monte Carlo simulations of the known $1p$ decays of the ground and first excited states of ^{15}F with $1p$ decay energies of 1.56(13) and 2.85(4) MeV, respectively [12]. The dash-dotted and dash-dot-dotted curves show the result of fits to the p-^{14}O correlation, indicating unknown excited states in ^{15}F with $1p$ decay energies of 4.9(2) and 6.4(2) MeV, respectively. The solid line is the sum fit.

of ^{19}Mg (see Figs. 2 and 4 in Ref. [9] and the respective discussions).

For the $2p$ decay of ^{16}Ne, the angular correlations of each coincident proton with respect to the ^{14}O momentum, θ_{p1-O}-θ_{p2-O}, derived from the measured $^{14}O + p + p$ coincidence events, are shown in Fig. 3(a). The events with the smallest angles fall into a distinct cluster around $\theta_{p-O} = 35$ mrad, while most of the other events are located in the slices centered around 70 and 95 mrad. These two groups can be attributed to the direct $2p$ decay from the ^{16}Ne ground state and to the sequential emission of protons from excited states in ^{16}Ne via the ^{15}F ground state, respectively. We shall refer to these events as the "ground state" and "excited state" events, respectively. The latter group also includes events resulting from the fragmentation reaction $^{17}\text{Ne} \rightarrow {}^{14}O + p + p + n$.

To disentangle the ground state from the excited state events, we made a slice projection from the measured (p_1-^{14}O)-(p_2-^{14}O) correlations in Fig. 3(a) by selecting the angle of one of the protons within the range 0–45 mrad, where the $2p$ decay of the ^{16}Ne ground state is expected to show up. Figure 3(b) displays the angular correlations θ_{p1-O} corresponding to the ground-state gate in the other pair θ_{p2-O}. The peak around 35 mrad (the suggested ground state) dominates the spectrum, whereas few correlations can be seen between a proton from the ground state and another proton at larger angles. This means that the two protons from the ground state are correlated; i.e., this peak can be explained by an emission of protons from the ground state in ^{16}Ne.

For a more quantitative analysis, the data are compared with a Monte Carlo simulation of the response of our setup to the direct $2p$ decay $^{16}\text{Ne} \rightarrow {}^{14}O + p + p$ with the known $2p$-decay energy of 1.4(1) MeV [11] by using the GEANT program [25]. The simulations took into account the above-mentioned experimental accuracies in tracking the fragments and in reconstructing the vertices as well as a low-angle cutoff due to the finite cluster width of a HI hit in MSD which does not allow one to distinguish protons and HI below about a 10 mrad opening angle. The normalized simulation reproduces the data in the low-angle peak very well. Fitting the $2p$-decay energy of ^{16}Ne in the same way as for ^{19}Mg [9], we find $Q_{2p} = 1.35$ (8) MeV, in very good agreement with the literature value of 1.4(1) MeV [11]. The contribution from the "tail" of the higher states to the ground-state peak amounts to about 20%. The shape of this distribution is assumed to have the same shape as the θ_{p1-O} distribution selected within the θ_{p2-O} range just outside the ground-state region, from 48 to 160 mrad (the dotted curve).

Figure 3(c) displays an example of an angular p-^{14}O distribution for "excited states" obtained from Fig. 3(a) by selecting the angular range of the other proton from 120 to 150 mrad, which corresponds to broad high-energy continuum states in ^{16}Ne decaying to ^{14}O via the low-lying states in ^{15}F. The Monte Carlo simulation of known one-proton decays $^{15}\text{F} \rightarrow {}^{14}O + p$ of the ground and first excited states in ^{15}F with $1p$-decay energies of 1.56(13) and 2.85(4) MeV [12] reproduces well the two smallest-angle peaks. The two higher-lying peaks indicate $1p$ decays of unknown excited states in ^{15}F with derived $1p$-decay energies of 4.9(2) and 6.4(2) MeV. The excited states in ^{19}Mg, ^{16}Ne, ^{18}Na, and ^{15}F will be addressed elsewhere.

We turn now to the discussion of angular p-p correlations following $2p$ decays. When the spin degrees of freedom are neglected and the total decay energy E can be considered as fixed, the three-body correlations are completely described by two variables. A convenient choice is an energy-distribution parameter E_{p-p}/E (where E_{p-p} is the relative energy between two protons) and an angle θ_k between the relative momenta of the fragments. Figure 4 shows such distributions predicted by the three-body model for the $2p$ decay of ^{19}Mg [18,19]. The three-body model predicts a distinctive correlation pattern

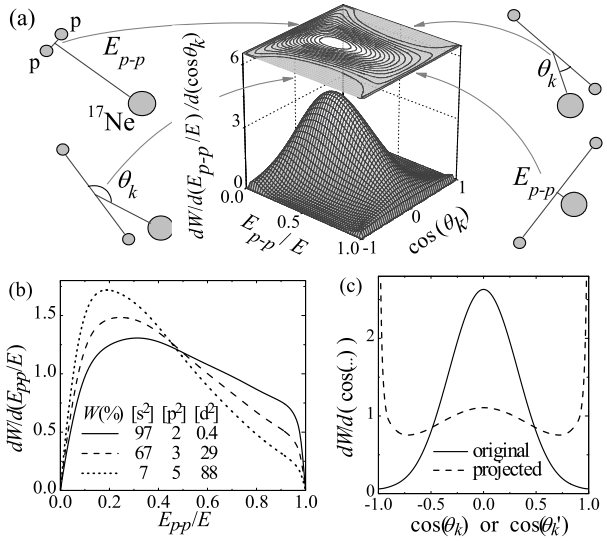

FIG. 4. (a) Three-body correlations predicted by the three-body model [19] for the $2p$ decay of ^{19}Mg, plotted as a function of the relative energy between two protons, E_{p-p}/E, and the angle θ_k between the relative momenta of the fragments as illustrated in the figure. Extreme cases of p-p correlations are sketched and related to the corresponding areas in the correlation plot. (b) p-p energy spectra from the $2p$ decay of ^{19}Mg calculated for different weights W of spd-shell configurations in ^{19}Mg. (c) Typical intensity distributions plotted as a function of θ_k [see (a)] in the rest frame of the $2p$ precursor (solid curve) and its analog in the laboratory system θ_k' projected on the transverse detector plane (dashed curve).

which features an enhancement at small E_{p-p} due to final-state interaction and a suppression in the regions of strong Coulomb repulsion ($E_{p-p}/E \sim 0.5, \cos(\theta_k) \sim \pm 1$). The predicted energy distributions are sensitive to the structure of the precursor [Fig. 4(b)]. Similar predictions are available for ^{16}Ne [20].

In our experiment, we were able to measure the opening angles θ_{p-p} between protons whose distribution reflects the

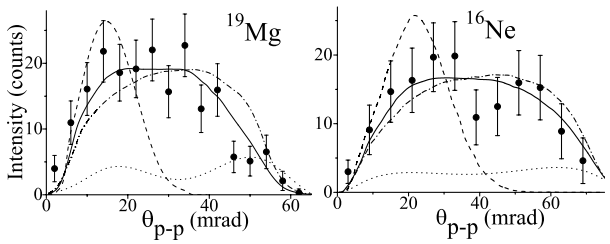

FIG. 5. Angular p-p correlations from the $2p$ decays of the ground states of ^{19}Mg (left) and ^{16}Ne (right) obtained from the measured ^{17}Ne$+p+p$ and ^{14}O$+p+p$ events, respectively, by selecting both protons from the respective p-^{17}Ne(^{14}O) angular ranges. The solid curves show the three-body model calculations (54% and 88% of d-wave configuration in ^{16}Ne and ^{19}Mg, respectively) normalized to the data. The dotted curves show the background contributions estimated as described in the text. The dashed curves are the diproton model predictions, and the dash-dotted curves are the phase-space simulations of the $2p$ decays (isotropic proton emission in the $2p$ precursor's rest frame).

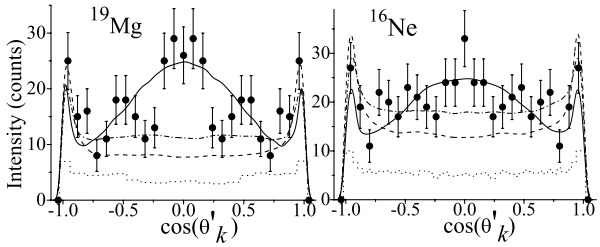

FIG. 6. Three-body correlations from the $2p$ decays of the ground states of ^{16}Ne and ^{19}Mg (full circles with statistical uncertainties) obtained from the measured ^{14}O $+ p + p$ and ^{17}Ne $+ p + p$ events by selecting an angle θ_k' (see text). The solid curves are the three-body model calculations (assuming 54% and 88% of d-wave configuration in ^{16}Ne and ^{19}Mg, respectively). The dashed curves are the diproton model predictions, and the dash-dotted curves are the phase-space simulations illustrating the response to an isotropic $2p$ emission in the precursor's rest frames (both simulations are not normalized). The dotted curves show the background contributions estimated from all measured HI $+ p + p$ events.

E_{p-p} correlations. Figure 5 shows the experimental angular p-p distributions obtained from triple ^{14}O$+p+p$ and ^{17}Ne $+ p + p$ events gated by the conditions that both protons originate from the ground states of ^{16}Ne and ^{19}Mg. These gates were inferred from the respective angular p-HI correlations as discussed above. The events representing the ground-state $2p$ decay actually contain contributions from the ground state and background contributions from excited states of both the parent nucleus and the fragmentation reactions. We evaluated the shapes of the background components empirically by projecting triple events with the p-HI gates shifted away from the "ground-state" region toward larger angles. The resulting p-p background contributions shown by the dotted curves in Fig. 5 constitute about 20% of all p-p correlation data for ^{16}Ne and 25% for ^{19}Mg (see Figs. 3(b) and 4(c) in Ref. [9]); they were subtracted from the original p-p correlations. As one can see in Fig. 5, the predictions following from the assumption of a diproton emission fail to describe both the ^{16}Ne and ^{19}Mg data, while the three-body model reproduces the shapes of both distributions. In the ^{19}Mg case, the best description is obtained with the d-wave configuration dominating. The ^{16}Ne data give evidence for nearly equal s- and d-wave components.

In Fig. 6, the intensity distributions are displayed as a function of $\cos\theta_k'$. The angle θ_k' [see Fig. 4(a)] was defined by a line connecting the two points where two protons hit the same detector and by a vector joining the middle between the $2p$ hits and the point of a related heavy-ion hit, in analogy with the angle θ_k shown in Fig. 4(a). The typical theoretical prediction for such a distribution is shown in Fig. 4(c). The diproton model predicts flat angular distributions in contrast to the experimental data in both cases. Only the three-body model can reproduce the characteristic shapes of the observed correlations with the broad bumps around $\cos\theta_k' = 0$ (the indicated spikes at $\cos\theta_k' \approx \pm 1$ predicted by all calculations are less conclusive). Such a shape is a manifestation of the "Coulomb focusing" efficiently repulsing the fragments from large regions of the momentum space [see Fig. 4(a)]. These distributions are weakly sensitive to the assumed structure of

the parent states but are an exclusive feature of the three-body model.

In summary, the measured three-particle correlations from the $2p$ decay of the ground states of ^{16}Ne and ^{19}Mg are described quantitatively by the predictions of the three-body model [19], in contrast to the quasiclassical diproton model which fails to describe our observations. These correlations are sensitive to the structure of the decaying nucleus. Thus the comparison between experiment and theory allows one to obtain spectroscopic information about the parent states. In ^{16}Ne, the data are consistent with strong s/d mixing [20]. In ^{19}Mg, the dominating d-shell configuration is the preferable description, which is also consistent with the lifetime information [9]. The method of measuring $2p$ decays in flight by precisely tracking all fragments with microstrip detectors provides new specific observables, thus yielding valuable spectroscopic information on such exotic isotopes. Information about two-body subsystems, e.g., ^{15}F, is simultaneously obtained. Systematic studies of other $2p$ emitters predicted theoretically [18,26] are foreseen with this novel technique.

The authors are grateful to M. Pohl and his co-workers of the DPNC, Université de Génève, for developing the microstrip detectors. We thank in particular E. Cortina for the valuable contribution to this project. We appreciate the help of A. Bruenle, K. H. Behr, W. Hueller, A. Kelic, A. Kiseleva, R. Raabe, and O. Tarasov during the preparation of the experiment. This work has been supported by contracts EURONS No. EC-I3 and FPA2003-05958, FPA2006-13807-C02-01 (MEC, Spain), the INTAS Grant 03-54-6545, the Russian RFBR Grants 05-02-16404 and 05-02-17535, and the Russian Ministry of Industry and Science Grant NS-1885.2003.2.

[1] V. I. Goldansky, Nucl. Phys. **19**, 482 (1960).
[2] I. Mukha *et al*., Nature (London) **439**, 298 (2006).
[3] O. V. Bochkarev *et al*., Nucl. Phys. **A505**, 215 (1989).
[4] R. A. Kryger *et al*., Phys. Rev. Lett. **74**, 860 (1995).
[5] C. R. Bain *et al*., Phys. Lett. **B373**, 35 (1996).
[6] B. V. Danilin, M. V. Zhukov, A. A. Korsheninnikov, L. V. Chulkov, and V. D. Efros, Sov. J. Nucl. Phys. **46**, 225 (1987) [Yad. Phys. **46**, 427 (1987)].
[7] A. A. Korsheninnikov, Sov. J. Nucl. Phys. **52**, 827 (1990) [Yad. Phys. **52**, 1304 (1990)].
[8] K. Miernik *et al*., Phys. Rev. Lett. **99**, 192501 (2007).
[9] I. Mukha *et al*., Phys. Rev. Lett. **99**, 182501 (2007).
[10] G. J. KeKelis *et al*., Phys. Rev. C **17**, 1929 (1978).
[11] C. J. Woodward, R. E. Tribble, and D. M. Tanner, Phys. Rev. C **27**, 27 (1983).
[12] A. Lepine-Szily *et al*., Nucl. Phys. **A734**, 331 (2004).
[13] W. A. Peters *et al*., Phys. Rev. C **68**, 034607 (2003).
[14] V. Z. Goldberg *et al*., Phys. Rev. C **69**, 031302(R) (2004).
[15] T. Zerguerras *et al*., Eur. Phys. J. A **20**, 389 (2004).
[16] L. V. Grigorenko, R. C. Johnson, I. G. Mukha, I. J. Thompson, and M. V. Zhukov, Phys. Rev. Lett. **85**, 22 (2000).
[17] L. V. Grigorenko, R. C. Johnson, I. G. Mukha, I. J. Thompson, and M. V. Zhukov, Phys. Rev. C **64**, 054002 (2001).
[18] L. V. Grigorenko and M. V. Zhukov, Phys. Rev. C **68**, 054005 (2003).
[19] L. V. Grigorenko, I. G. Mukha, and M. V. Zhukov, Nucl. Phys. **A713**, 372 (2003); **A740**, 401(E) (2004).
[20] L. V. Grigorenko, I. G. Mukha, I. J. Thompson, and M. V. Zhukov, Phys. Rev. Lett. **88**, 042502 (2002).
[21] A. M. Lane and R. G. Thomas, Rev. Mod. Phys. **30**, 257 (1958).
[22] A. I. Baz', V. I. Goldansky, V. Z. Goldberg, and Ya. B. Zeldovich, *Light and Intermediate Nuclei Near the Border of Nuclear Stablity* (Nauka, Moscow, 1972).
[23] H. Geissel *et al*., Nucl. Instrum. Methods Phys. Res. B **70**, 286 (1992).
[24] http://dpnc.unige.ch/ams/GSItracker/www/.
[25] "GEANT - detector simulation tool", CERN software library, http://wwwasd.web.cern.ch/wwwasd/geant.
[26] L. V. Grigorenko, I. G. Mukha, and M. V. Zhukov, Nucl. Phys. **A714**, 425 (2003).